On-chip fabrication to add temperature control to a microfluidic solution exchange system

On-chip fabrication to add temperature control to a microfluidic solution exchange system†

Helen Bridle, Maria Millingen and Aldo Jesorka*

Received 30th November 2007, Accepted 19th December 2007
First published as an Advance Article on the web 25th January 2008
DOI: 10.1039/b718368b

We present a concept for the post production modification of commercially available microfluidic devices to incorporate local temperature control, thus allowing for the exact alignment of heating structures with the existing features, *e.g.* wells, channels or valves, of a system. Specifically, we demonstrate the application of programmable local heating, controlled by computerized PI regulation, to a rapid solution exchanger. Characterisation of the system to show that both uniform temperature distributions and temperature gradients can be established, and to confirm that the solution exchange properties are undisturbed by heating, was achieved using *in situ* thermometry and amperometry.

Introduction

We demonstrate a post production fabrication method to add local temperature control to a commercially available microfluidic device, optimized for patch-clamp based ion channel studies.[1,2] This microfluidic system creates a patterned laminar flow in an open volume *via* the viscous coupling of flows exiting an array of microchannels.[3] A cell, scanned through the patterned flow, close to the channel outlets, experiences millisecond solution exchange between the separate solution environments in the flow.[3,4] Programmable temperature control is obtained *via* resistive heating and an *in situ* microthermocouple. Heating is applied only to the area outside the channel outlets, since experiments are performed here. Additionally, local heating is both rapid and avoids unnecessary exposure of other cells and solutions stored on chip to high temperatures. Deposition of the heating structures post assembly of the device allows for accurate alignment between the structures and the channel outlets, which is essential to obtain a uniform temperature distribution.

This modified system is ideal to study ion channels, as it offers the combination of both chemical and temperature control. This is useful for many different reasons: to ensure the physiological relevance of the results, which is especially important in toxicological testing; to study heat-activated ion channels, specifically those which are also ligand-gated; and to obtain kinetic and thermodynamic information. The system has been applied to show, using the $GABA_A$ receptor, that EC_{50} values can exhibit different temperature dependence for different ligands.[5]

In this paper, we show how our modified system can be operated to achieve either a uniform homogeneous temperature distribution across the channels or a temporal temperature gradient. Furthermore, we show that the laminar flow pattern, and thus the solution exchange characteristics, is maintained at different temperatures. Additionally, we describe the key elements in the fabrication procedure that can, with appropriate modifications to tools and processes, be adapted for other commercially available microfluidic systems or research prototypes, in principle even without a dedicated cleanroom environment.

Experimental

The microfluidic rapid solution exchanger and heating set-up

We employed a microfluidic chip from Cellectricon AB, Gothenburg, Sweden. A detailed description of the chip can be found elsewhere[1,3,6,7] and in the ESI.† In brief, it comprises 16 microchannels, originating in individual solution reservoirs, that exit as a tightly packed array into an open volume.[3] The heating structure is placed at the area where the channels exit into the open volume (Fig. 1A, S1).† A microscope stage holder was designed, containing 2 pivot connectors (Fig. S1A†, S2B†, S2C†) which connect the gold strips emanating from the heating structure to a voltage source for resistive heating. The system also features an *in situ* microthermocouple for temperature measurement, as well as a programmable control interface for feedback (Fig. S1A).†

Microfabrication of the heating structure

Thin metal film heating structures are deposited onto the glass underside of the chip by a standard photolithographic process, followed by resistive vapour deposition and lift-off of the resist (Fig. 1B). Shipley S1813 is spin-coated onto the glass underside of the chip. Subsequently, the chip is placed in the mask aligner (Karl Suss) and exposed to UV for 10 s through a mask outlining the heating structure. For the particular microfluidic system we target, a simple modification to the spinner/mask aligner chuck was devised in order to accommodate the non-planar geometry of the chip (Fig. S3A).† Development of the exposed

Department of Chemistry and Bioscience and Microtechnology Centre, Chalmers University of Technology, SE-412 96, Göteborg, Sweden. E-mail: aldo@chembio.chalmers.se; Fax: +46 (0)31 772 61 20; Tel: +46 (0)31 772 61 12

† Electronic supplementary information (ESI) available: Supplementary Figures S1–S10 and Table S1. See DOI: 10.1039/b718368b

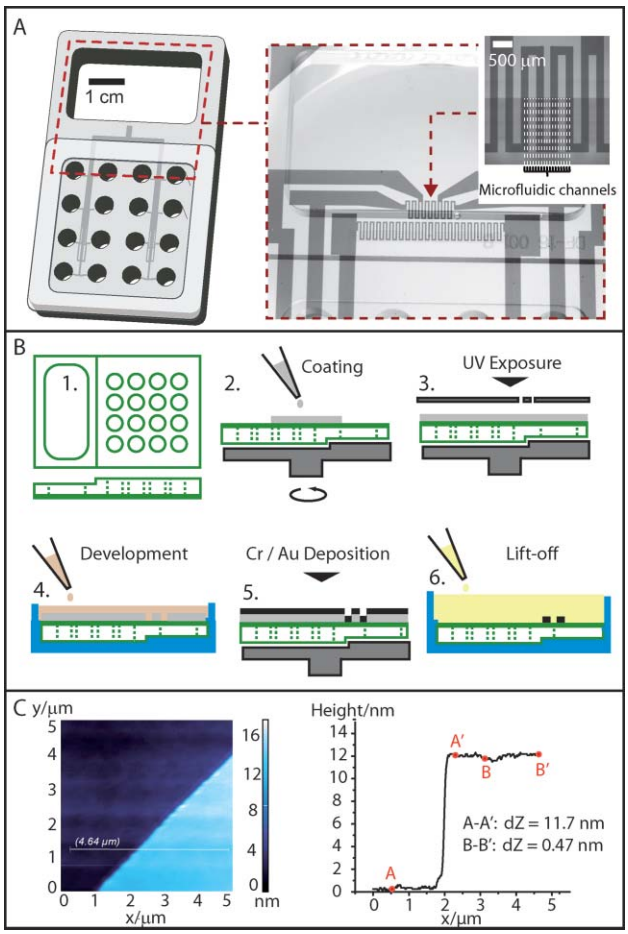

Fig. 1 Design, fabrication and characterisation of the heating structures. (A) Left: top view of the microfluidic chip. Right: the heating structure is deposited on the glass underside of the chip and is positioned so that it covers the channel outlets (inset). Both the width of and the spacing between the turns in the coil are ~200 µm. The width of the channel array is 1130 µm and the middle 2 loops of the heating coil are aligned to the channel array. The height of the coils is 2 mm and they are situated so that 1 mm covers the array of channels before the outlets and 1 mm covers the flow pattern in the open volume. (B) Schematic of the fabrication procedure. (C) Left: atomic force micrograph of the surface across the edge of 1 coil. The coloured panel indicates the height in nm. Right: height profile across the edge of one structure along the line shown in the left image. The height step (A-A′) is ~11 nm, in accordance with the metal evaporation protocol used for the fabrication, whereas the uniformity (B–B′) within the film is less than 1 nm.

resist is achieved using a fitting metal enclosure around the chip, which only exposes the rectangular glass surface to the developer (Fig. S3B).† The elastic PDMS effectively seals the enclosure and avoids contamination of the channels and sample wells. Following development, the chip is blow-dried with air, plasma cleaned in an oxygen plasma for 15 s (RIE batchtop plasma chamber, 50 W RF power and 10 sccm O_2 at 250 mtorr pressure) and a 3.5 nm Cr adhesion layer and a 7.5 nm Au layer is evaporated onto the glass. Lift-off is performed in Shipley 1165 resist remover, using again an enclosing case around the chip to avoid contamination of the channels and sample wells (Fig. S3C).† Standard workshop procedures are sufficient for production of these special tools since high precision machining is not required. AFM measurements were performed on a NT-MDT Integra instrument in the semi-contact mode.

Characterisation experiments

In order to characterize the temperature distribution at the channel outlets, an in-house built microprobe,[8,9] with a spherical thermocouple having a diameter of 50 µm, was scanned from channel 1 to 16 while the temperature was sampled. To measure concentration profiles within the laminar flow pattern, amperometric scans were performed as described previously.[6] Further details of the characterisation experiments can be found in the ESI.†

Results and discussion

On chip fabrication

To investigate the reproducibility of the fabrication process, six thin film heaters were fabricated under identical conditions and the U-I-R characteristics determined using a parameter analyzer (Fig. S5).† The mean resistance for the series was calculated as 1529.1 Ohms with a standard deviation of 29.7 Ohms (see Table S1).† To confirm film quality, AFM was performed and showed that the film is essentially flat within 1 nm and remains defect free (Fig. 1C, S6).† Film edges show slightly irregular height characteristics, which is due to the simplified lithography without a lift-off layer. Given the large dimensions of the film structures, these edge effects are not relevant for proper function.

To maintain optical transparency, a metal film thickness of less than 15 nm is required. This results in relatively high voltage requirements (in the range of 15–40 volts) for heat generation. However, it is no problem to achieve such voltages in our system (Fig. S5).† For lower voltage requirements, optically, highly transparent ITO surfaces could be utilized instead of metal films. However, deposition of ITO structures with sufficient quality is comparatively complicated and while wet-etching of commercially available pre-sputtered glass is possible, such substrates are excessively expensive. Moreover, thermal decomposition of ITO and resulting loss of function is much more severe at higher temperatures[10] than for evaporated metal films.

Characterisation of the system

Application of a large step change in the voltage to the resistive heating structures results in a maximum heating rate of 22 °C s^{-1}. However, to achieve controlled temperature steps without overshoots and oscillations, the proportional/integral (PI) feedback mode was used with optimised PI parameters, resulting in a time for heating 25 °C to 50 °C of ~21 s (Fig. S7).† There is no method of cooling, so decreases in temperature rely entirely upon heat dissipation but since the chip is only locally heated, this process also occurs on the order of tens of seconds (Fig. S7).†

Feedback from the thermocouple to the voltage source allows for rapid adjustment of the temperature at the position where the thermocouple is located and can be used to compensate for any spatiotemporal variations in temperature. However, when performing patch-clamp experiments with this system, the cell cannot be placed within ~300 µm of the thermocouple and

thus feedback will not ensure that the cell experiences a uniform temperature during a scan across the channel outlets (see the ESI† for further discussion). To confirm that a spatially uniform temperature distribution was obtained across the channel outlets, even without feedback, at the standard position where the cell is scanned (25 μm outside the channel outlets and 30 μm above the bottom of the chip), the thermocouple was scanned, at this position, while sampling the temperature. As shown in Fig. 2A, the uniformity of the temperature across the channel outlets is within ±0.2 °C. Over time, a slight upward drift of temperature is observed, though this is less than ±0.2 °C for 60 s for all temperatures studied (Fig. S8).† Furthermore, the local nature of the heating was confirmed by performing scans out into the open volume (Fig. S9).† The feedback can be employed to create temporal gradients (Fig. 2B, C). The ability to change between different temperatures is important for studies on heat activated ion channels, *e.g.* in order to determine the temperature threshold for activation.

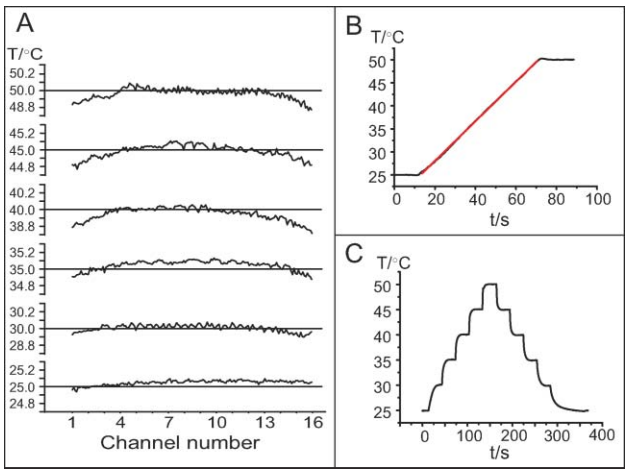

Fig. 2 Thermocouple measurements. (A) Stability of the temperature over all 16 channels in the standard position. At all 6 temperatures, the uniformity of the temperature across the channel outlets is within ±0.2 °C. The black horizontal lines show the desired temperature. Note that the *y* axis is discontinuous. (B) A linear gradient between 25 °C and 50 °C over 60 s. The red line shows a linear fit to the data, T (°C) = 19.47(°C) + 0.42941(°C s^{-1})·t(s) with an R value of 0.99983. When creating the linear gradient, going from 25 °C to 50 °C in 60 s, the PI parameters of the feedback mode needed to be continuously adjusted in order to avoid too slow initial heating. Therefore, the P parameter was allowed to vary, starting from a large value and then decreasing exponentially. (C) Using the PI feedback, and constant parameters, the temperature was increased from 25 °C to 50 °C and back to 25 °C in 5 °C increments.

Heating may disturb the flow pattern *via* several different effects. Firstly, convection due to heating has been observed in similar heating systems (M. Markström, personal communication). However, such systems were static, while in our system the liquid is moving as a laminar flow. Secondly, formation of air bubbles, nucleated at the channel outlets, was initially observed at ≥50 °C. This was easily avoided by degassing the chip in a dessicator prior to experiments, allowing heating to 90 °C without formation of bubbles. Thirdly, the diffusion zone width may be altered since the diffusion coefficient changes with temperature. Calculations predicted an increase in interface width from 10 μm to 13 μm between 25 °C and 50 °C at 25 μm from the channel outlets (see ESI†), which could lead to slower exchange times at higher temperatures.[11] We utilised amperometry to confirm that the flow exiting the channels still forms a laminar pattern and to characterise the interface between adjacent solution segments at 6 different temperatures between 25 °C and 50 °C and at 3 different distances from the channel outlets (Fig. 3). The results show that, at 25 μm from the channel outlets, there is only a very small difference between the scans at different temperatures, indicating that any change in the interface width is negligible. Thus, it is expected that the solution exchange times remain comparable at different temperatures.

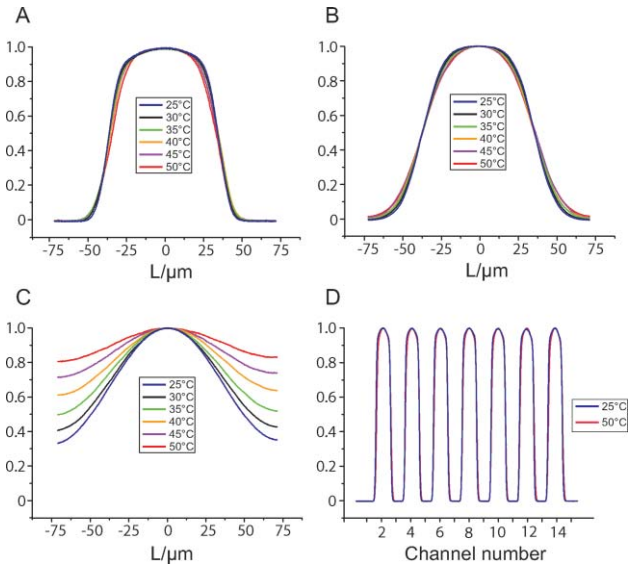

Fig. 3 Amperometry measurements showing the concentration profiles in the laminar flow. The *y* axes show the normalised current, corresponding to concentration. The *x* axes in A–C indicate the distance from the centre of channel 6. (A) A scan, at 25 μm from the channel outlets from the mid-point of channel 5 to the mid-point of channel 7, where channels 5 and 7 are loaded with buffer and channel 6 contains 100 μM hexaammineruthenium (III) chloride. (B) and (C), the same experiment repeated for the distances 100 μm and 250 μm, respectively, from the channel outlets. (D) Comparison of complete scans at 25 μm across all 16 channels loaded alternately with buffer and 100 μM hexaammineruthenium (III) chloride for 25 °C and 50 °C. All traces are normalised.

Conclusion

We have described a post-production on-chip fabrication method to add local temperature control to commercially available microfluidic devices. Specifically, we demonstrated addition of programmable temperature control to a microfluidic system for rapid solution exchange applications and showed that a uniform temperature distribution over the channel outlets can be achieved, without disruption of the solution exchange properties. Additionally, we have demonstrated how the system can be used to obtain different temporal temperature gradients. The fabrication method produces thin-film heating structures of reproducible resistance and can, in principle, be performed outside a cleanroom facility. The method is easily adapted for the modification of other systems and offers the advantage of

exact alignment of heating structures to existing features, *e.g.* channels, wells or valves.

Acknowledgements

This work was supported by the Swedish Research council (VR), the Swedish Foundation for Strategic Research (SSF), the Nano-X, and Biomics programs, and the Göran Gustafsson Foundation.

References

1 J. Sinclair, J. Pihl, J. Olofsson, M. Karlsson, K. Jardemark, D. T. Chiu and O. Orwar, *Anal. Chem.*, 2002, **74**, 6133–6138.
2 www.cellectricon.se.
3 J. Olofsson, J. Pihl, J. Sinclair, E. Sahlin, M. Karlsson and O. Orwar, *Anal. Chem.*, 2004, **76**, 4968–4976.
4 D. Granfeldt, J. Sinclair, M. Millingen, C. Farre, P. Lincoln and O. Orwar, *Anal. Chem.*, 2006, **78**, 7947–7953.
5 M. Millingen, H. Bridle, A. Jesorka, P. Lincoln and O. Orwar, *Anal. Chem.*, 2008, **80**, 340–343.
6 J. Olofsson, H. Bridle, J. Sinclair, D. Granfeldt, E. Sahlin and O. Orwar, *Proc. Natl. Acad. Sci. U. S. A.*, 2005, **102**, 8097–8102.
7 J. Sinclair, D. Granfeldt, J. Pihl, M. Millingen, P. Lincoln, C. Farre, L. Peterson and O. Orwar, *J. Am. Chem. Soc.*, 2006, **128**, 5109–5113.
8 J. D. Nash, D. R. Caldwell and M. J. Zelman, *J. Atmos. Ocean. Technol.*, 1999, **16**, 1474–1482.
9 M. Markström, A. Gunnarsson, O. Orwar and A. Jesorka, *Soft Matter*, 2007, **3**, 587–595.
10 S. Gardonio, L. Gregoratti, P. Melpignano, L. Aballe, V. Biondo, R. Zamboni, M. Murgia, S. Caria and A. Kiskinova, *Org. Electron.*, 2007, **8**, 37–43.
11 F. Sachs, *Biophys. J.*, 1999, **77**, 682–690.